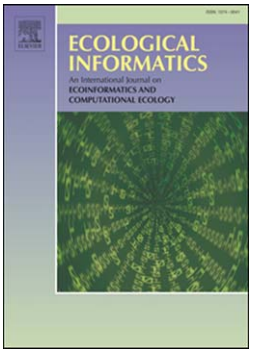

Effects of altered precipitation regimes on plant productivity in the arid region of northern China

Hao-jie Xu, Xin-ping Wang

PII: S1574-9541(15)00199-5
DOI: doi: 10.1016/j.ecoinf.2015.12.003
Reference: ECOINF 645

To appear in: *Ecological Informatics*

Received date: 9 September 2015
Revised date: 2 December 2015
Accepted date: 9 December 2015

Please cite this article as: Xu, Hao-jie, Wang, Xin-ping, Effects of altered precipitation regimes on plant productivity in the arid region of northern China, *Ecological Informatics* (2015), doi: 10.1016/j.ecoinf.2015.12.003

Effects of altered precipitation regimes on plant productivity in the arid region of northern China

Hao-jie Xu[a,b], Xin-ping Wang[a]

a Shapotou Desert Research and Experiment Station, Cold and Arid Regions Environmental and Engineering Research Institute, Chinese Academy of Sciences, Lanzhou 730000, China

b University of Chinese Academy of Sciences, Beijing 100049, China

Corresponding author:

Dr. Xin-ping Wang

Tel: +86-931-4967183

Fax: +86-931-8273894

E-mail: xpwang@lzb.ac.cn

Abstract： Climate change scenarios have predicted significant alterations in precipitation patterns over most of the mid-latitude land areas by the end of this century, but the degree to which altered precipitation regimes influence terrestrial ecosystem function in arid regions is uncertain. Precipitation is a primary climatic factor that regulates ecosystem function in arid regions. Based on remote sensing and meteorological data from 2000 to 2013, we analysed the spatiotemporal variations in annual net primary productivity (NPP) for different land cover types in the arid region of northern China and quantified the effects of growing season precipitation (GSP) and seasonal distribution of precipitation (SDP) on NPP variability by using the ecological process CASA (Carnegie–Ames–Stanford Approach) model. Our results suggested that significant NPP increases were found in most of the vegetated areas, especially in grasslands and shrublands. Responses of NPP to precipitation variability were related to land cover types. Grassland and shrubland were most responsive to precipitation variability followed by croplands and forests. Increased precipitation increased NPP, and NPP responded more strongly to higher precipitation than lower precipitation. We also found that increased precipitation concentration decreased NPP. GSP and SDP accounted approximately 67% and 21% of the variability in NPP. We concluded that growing season precipitation and its seasonal distribution were dominant factors controlling inter-annual variability in NPP in the arid region of northern China. Other factors, such as plant functional trait, antecedent soil moisture and human activities, might mediate NPP responses to precipitation variability through interaction with water availability. Our studies have implications for assessing and predicting vegetation responses to future climate change.

Keywords： Net primary productivity; Climate change; Precipitation quantity; Seasonal distribution of precipitation; Arid region; northern China

1. Introduction

The accelerating water cycle in consequence of global warming is forecasted to bring about dramatic changes in precipitation regimes over most of the mid-latitude land areas by the end of this century, although there may be regional exceptions (Easterling et al., 2000). The predicted changes in precipitation regimes are characterized by larger precipitation events with longer dry intervals (Knapp et al., 2008). There is mounting evidence that more extreme intra-annual precipitation regimes, such as alterations in the seasonal distribution of precipitation and increasing extreme precipitation events in the 99^{th} percentile of intensity within and across seasons (Kunkel et al., 1999), may exert a more profound impact on the temporal variability of soil moisture at different soil depths than changes in annual average precipitation (Schwinning and Sala, 2004). This may have ecological and evolutionary implications for water use strategies of plants (Weltzin et al., 2003). Water is an important driver of biological processes (i.e., species reordering, community assembly and

biogeochemical cycling) in arid regions (Noy-Meir, 1973), where episodic precipitation inputs are the main water source, and water availability dominates the dynamics of microbes, plants and entire ecosystems (Reyer et al., 2013). Net primary productivity (NPP), the net gain in biomass by vegetation through photosynthesis, is an indicator of ecosystem function and plays a crucial role in regulating ecosystem carbon balance (Pettorelli et al., 2012). Indeed, understanding how altered precipitation regimes influence terrestrial ecosystem productivity may broaden our knowledge of terrestrial carbon cycle in response to potential climate perturbations (Schimel et al., 2001).

Historical studies have substantiated that mean annual precipitation is a robust predictor of NPP over large spatial and temporal scales (Knapp and Smith, 2001), and the inter-annual variability in NPP is related to fluctuations in precipitation (Fang et al., 2001). In recent years, an increasing interest in the effects of more extreme intra-annual precipitation patterns on plant productivity has spurred on extensive research through environmentally controlled field experiments and ecological modelling (Smith, 2011). Whether altered precipitation regimes, including changes in magnitude, frequency and timing, lead to increased or decreased NPP in arid and semiarid regions depends on the impact of precipitation upon plant available water (Zeppel et al., 2014). High precipitation intensity with long intervening periods between precipitation events suggests more concentrated precipitation distribution (Guo et al., 2008), which may recharge deeper soil layers further effectively but deplete upper soil layers more severely than ambient precipitation patterns (Knapp et al., 2008). The two-layer soil water-partitioning hypothesis predicts that such redistribution of soil moisture is expected to favour the growth of deep-rooted woody plants but to depress the growth of shallow-rooted herbaceous plants (Walter, 1971). Most field data derived from experimental precipitation manipulations suggest that increased precipitation concentration decreases NPP in semiarid regions (Fay et al., 2008; Hoover et al., 2014), whereas increased precipitation concentration increases NPP in arid regions (Baez et al., 2013; Muldavin et al., 2008). In addition to variability in precipitation magnitude and frequency, the timing of precipitation variability may differentially affect NPP at different stages throughout the year, depending on whether soil moisture controls plant growth over that period (Craine et al., 2012). For example, more precipitation in spring and summer may have stronger positive effects on plant growth than that in autumn and winter (Bates et al., 2006).

Despite the growing recognition of the vital importance of precipitation variability to the dynamics of terrestrial vegetation ecosystems, much of our basic understanding about ecological responses to altered precipitation regimes is gained from field manipulative experiments (Knapp et al., 2008; Smith, 2011). This results in enormous difficulties in establishing the relationship between NPP and precipitation anomalies at a broad scale due to small sample size locally and large spatial variations of NPP (Fang et al., 2001). Moreover,

recent researches into the effect of the variability and extremes in precipitation on plant growth are undertaken mainly in semiarid and semihumid regions, where mean annual precipitation varies from 250 mm to 800 mm (Heisler-White et al., 2008). However, how vegetation in arid regions with total precipitation less than 250 mm respond to altered precipitation regimes remains largely unknown (Robertson et al., 2009). As the precipitation variability and precipitation amount are correlated, it is difficult to evaluate the effect of precipitation variability on plant productivity (Knapp and Smith, 2001).

Most previous studies analysed NPP responses to altered precipitation regimes at local scales (Heisler-White et al., 2008; Hoover et al., 2014; Muldavin et al., 2008), few studies focused on the relationships between NPP and intra-annual variations in precipitation at regional scales (Fang et al., 2001). Moreover, the way by which altered precipitation regimes affected NPP variability was not adequately explored as different vegetation types might have diverse responses to variability in precipitation (Vicente-Serrano et al., 2013). In this study, we focused on the spatiotemporal variations in annual NPP for different land cover types and assessed the impacts of growing season precipitation (GSP) and seasonal distribution of precipitation (SDP) on NPP in the arid region of northern China. The study area was defined as the region receiving mean annual precipitation less than 250 mm over the period of 1961-2010. SDP was defined as a measure of the evenness of distribution of monthly precipitation within the growing season (Guo et al., 2012). We assumed that the effect of GSP and SDP on ecosystem function such as NPP might vary for different land cover types. Other ecological factors might mediate NPP responses to precipitation variability and explain regional differences in the relationship between NPP and precipitation anomalies (Ogle and Reynolds, 2004). Our primary goal was to analyse the inter-annual variations in annual NPP at regional scales and determine the relative importance of GSP and SDP to variability in NPP for different land cover types. This study may be helpful on agriculture water management and ecological protection in arid regions under likely future scenarios of more extreme precipitation events (Valipour, 2015a, 2014).

2. Materials and methods

2.1 Study area

The arid region of northern China (36°26′–48°54′ N, 73°56′–117°43′ E) is located in the north of the Qinghai-Tibet Plateau with a total area of approximately 1.76×10^6 km^2 (Fig. 1). It comprises the Junggar Basin, Tarim Basin, Turpan Depression, Hexi Corridor, Alxa Plateau, Ulanqab Plateau, Xilingol Plateau and Hulun Buir Plateau. This region has a typical temperate continental climate with a wide annual range of temperature and precipitation (Yang et al., 2010). According to the long-term climate records over the period of 1961-2010, mean annual temperature is 8.7 °C, with the lowest temperature of -10.8 °C in January and

the highest of 28.8 °C in July. Mean annual precipitation is 107.5 mm, 86.3 % of which occurs from April to October, and average annual potential evapotranspiration is approximately 1097.7 mm (Mao et al., 2014). The major land cover types include forests, shrublands, grasslands and croplands, which account for 0.06 %, 11.1%, 15.1 % and 1.9 % of the total study area, respectively (Fig. 1). Woody plant communities comprise mainly *Populus euphratica*, *Calligonum arborescens*, *Tamarix chinensis*, *Haloxylon ammodendron* and *Reaumuria soongorica*. Herbaceous plant communities are dominated largely by *Stipa klemenzii*, *Agropyron desertorum*, *Cleistogenes songorica*, *Artemisia frigida* and *Potentilla chinensis* (Ma et al., 2008). Maize and wheat are the most widely grown grain crops throughout the study area. The soil types shift from calcic brown and sierozem soils to desert soils from the east to the west, with decreases in soil moisture and organic content (Guo et al., 2012).

Figure 1 here

2.2 Datasets

The Normalized Difference Vegetation Index (NDVI) dataset derived from measurements taken by the Moderate Resolution Imaging Spectroradiometer (MODIS) sensor was utilized to estimate NPP at a regional scale (Mao et al., 2014; Zhang et al., 2014). The 16-day composition MODIS NDVI product (MOD13A2) with a spatial resolution of 1 km from 2000 to 2013 was obtained from the Land Processes Distributed Active Archive Centre (https://lpdaac.usgs.gov). The MODIS NDVI dataset was corrected for calibration, view geometry and atmospheric correction (Fensholt et al., 2009). To have high-quality NDVI time series, a Savitzky-Golay smoothing filter was employed to reduce the residual noise caused by haze and clouds (Chen et al., 2004). Monthly MODIS NDVI dataset was created with the maximum value composite (MVC) method (Taddei, 1997).

In this study, monthly meteorological data including temperature, precipitation and solar radiation were collected from 72 permanent meteorological stations from 2000 to 2013 (Fig. 1). These data were available from the China Meteorological Data Sharing Service System (http://cdc.cma.gov.cn). The meteorological data except for precipitation were processed into raster layers at 1 km spatial resolution using bivariate thin plate smoothing splines, which incorporated varying degrees of dependence on topography, including both aspect and elevation (Hancock and Hutchinson, 2006). As the precipitation data were derived from a few gauges, it was difficult to obtain reliable precipitation patterns by using spatial interpolation methods for ground-based precipitation observations (Sun et al., 2015). Thus, we used monthly gridded Tropical Rainfall Measurement Mission (TRMM) product (TRMM 3B43) at 0.25° spatial resolution from 2000 to 2013, which was provided by the National Aeronautics and Space Administration (NASA) and the Japan Aerospace Exploration Agency (JAXA)

(http://trmm.gsfc.nasa.gov). The TRMM precipitation data were validated against gauge-based precipitation measurements (Fig. 2) and were resampled to grid cells with 1×1 km using a bilinear interpolation technique.

The aboveground biomass data, including alive and standing dead biomass produced in the current year, were collected from 85 field sample sites (60 grassland sites and 25 shrubland sites, Fig. 1). From 2001 to 2005, we measured the aboveground biomass of grasslands and shrublands in late July or August, when grassland and shrubland reached their peak aboveground biomass (Ma et al., 2008). The aboveground biomass data were used to confirm simulated NPP (Fig. 3). At each grassland site (10×10 m), the aboveground biomass in five quadrates (1×1 m) was measured. All biomass samples were oven-dried at 65 ℃ for 48 h to constant mass and were weighed to the nearest 0.1 g. More detailed procedures of the field investigation were introduced by Yang et al. (2010). At each shrubland sites (10×10 m), we categorized shrub plants into three groups in the light of their sizes (large, medium and small) and selected an exemplary plant in each group with its current-year leaves and twigs being harvested, oven-dried and weighed. The total weights of the three shrub groups were calculated by multiplying the weight of the representative plants by their quantities in each group (Zhao et al., 2014). Statistical analysis suggested that there was no significant difference between each biomass sample within a site. The aboveground biomass for each site was represented by averaging the weight of all biomass samples. To validate the results of simulated grassland and shrubland NPP, we assumed that aboveground biomass represented aboveground NPP and obtained an estimated ratio of aboveground to belowground NPP (Ma et al., 2008). Because of the difficulties in quantifying forest and cropland NPP, we used the MODIS NPP product (MOD17A3) to validate the results of simulated forest and cropland NPP. The annual composition MOD17A3 product with a spatial resolution of 1 km from 2000 to 2010 was derived from the Land Processes Distributed Active Archive Centre (https://lpdaac.usgs.gov). This product produced gross primary productivity (GPP) of vegetation every day and summed to NPP at the end of the year. A more detailed overview of the MODIS NPP algorithm was introduced by Zhao et al. (2005).

Other ancillary data included 1:250,000 scale administrative district map, 1:1,000,000 scale vegetation and soil maps, and digital elevation model (DEM). All the above data were resampled to match MODIS NDVI data at 1 km spatial resolution using a majority function in the Resample Tool of ArcGIS.

2.3 Methods

Based on MODIS NDVI data, temperature, precipitation and solar radiation data, in conjunction with vegetation type and soil texture information, the CASA (Carnegie–Ames–Stanford Approach) model was developed to simulate monthly NPP (Potter et al., 1999). The

annual NPP dataset was obtained by calculating accumulated monthly NPP in a year (Zhao et al., 2005). In the CASA model, NPP is determined with absorbed photosynthetically active radiation (APAR), multiplied by light utilization efficiency (ε). It is noteworthy that the effect of maintenance respiration (MR) is estimated by time-varying stress scalar terms for temperature and moisture behind the CASA algorithm logic (Potter et al., 1999).

$$NPP = GPP - MR = APAR \times \varepsilon = PAR \times fAPAR \times \varepsilon^{*} \times T_{\varepsilon} \times W_{\varepsilon} \quad (1)$$

Where PAR is the total incident photosynthetically active radiation (MJ/m^2) and accounts for 50% of total solar radiation. fAPAR is the fraction of PAR absorbed by photosynthetic tissues in a canopy. ε* is the maximum light utilization efficiency set as different constant values for different land cover types. In this study, ε* of forests, shrublands, grasslands and croplands was set to 1.004, 0.768, 0.608 and 0.604 g C/MJ, respectively (Zhu et al., 2006). T_{ε} and W_{ε} are time-varying stress scalar terms for temperature and soil water balance.

fAPAR is estimated from a linear function of NDVI following Myneni and Williams (1994).

$$fAPAR = \frac{(NDVI - NDVI_{min})(fAPAR_{max} - fAPAR_{min})}{(NDVI_{max} - NDVI_{min})} + fAPAR_{min} \quad (2)$$

Where $NDVI_{min}$ and $NDVI_{max}$ correspond to the 5th and 95th percentile of NDVI in each land cover type. $fAPAR_{min}$ and $fAPAR_{max}$ are set to 0.001 and 0.95.

T_{ε} is calculated concerning derivation of the optimal temperature (T_{opt}) for plant production.

$$T_{\varepsilon} = (0.8 + 0.02T_{opt} - 0.0005T_{opt}^{2}) \left(\frac{1.184}{1 + \exp\{0.2(T_{opt} - 10 - T)\}} \right) \left(\frac{1}{1 + \exp\{0.3(-T_{opt} - 10 + T)\}} \right) \quad (3)$$

Where T_{opt} is the monthly mean temperature (T) in the month of maximum NDVI.

W_{ε} is the monthly water deficit, which is simulated by a comparison of monthly actual evapotranspiration (ET) to monthly potential evapotranspiration (PET) from the method of Rahimi et al. (2015) and Yu et al. (2011).

$$W_{\varepsilon} = 0.5 + 0.5 \times \frac{ET}{PET} \quad (4)$$

$$ET = \frac{P \times Rn \times (P^2 + Rn^2 + P \times Rn)}{(P + Rn) \times (P^2 + R\,n^2)} \quad (5)$$

$$Rn = \sqrt{E_0 \times P} \times (0.369 + 0.589 \times \sqrt{\frac{E_0}{P}}) \quad (6)$$

$$E_0 = 16 \times (10 \times \frac{T}{I})^{\alpha} \quad (7)$$

$$\alpha = (0.675 \times I^3 - 77.1 \times I^2 + 17920 \times I + 492390) \times 10^{-6} \quad (8)$$

$$I = \sum_{i=1}^{12} (\frac{T}{5})^{1.514} \quad (9)$$

$$PET = \frac{ET + E_0}{2} \quad (10)$$

Where P is the monthly precipitation (mm). Rn is the net solar radiation (MJ/m^2). I is the total heat index in a year. Recent studies suggested that the used method for estimating potential evapotranspiration in this study was applicable and satisfactory (Valipour, 2015b, 2015c).

Based on the NPP simulation, further investigation was conducted to detect long-term annual NPP changing trend for each pixel by Eq. (11).

$$Slope = \frac{n \times \sum_{i=1}^{n} (i \times NPP_i) - \sum_{i=1}^{n} i \times \sum_{i=1}^{n} NPP_i}{n \times \sum_{i=1}^{n} i^2 - (\sum_{i=1}^{n} i)^2} \quad (11)$$

Where n is the sequential year. NPP_i is the annual NPP in the year i. A positive or negative slope value suggests a linear increasing or decreasing trend in NPP within the time (Chen et al., 2014). The F-test was applied to determine the significance level (p) of the trends in NPP. Based on the results of the significance test and the trend investigation, the trends were classified according to four ranks: significant increase (Slope $\geqslant$ 0 and $p \leqslant 0.05$), insignificant increase (Slope $\geqslant$ 0 and $p > 0.05$), significant decrease (Slope $<$ 0 and $p \leqslant 0.05$) and insignificant decrease (Slope $<$ 0 and $p > 0.05$). The total percentage change of annual NPP (TPC) as measured as the ratio of slope to the initial values following Ma and Frank (2006).

$$TPC = \frac{(n-1) \times Slope}{(1/n) \times \sum_{i=1}^{n} NPP_i} \quad (12)$$

In this study, GSP was defined as accumulated precipitation for the growing season (April to August). SDP was quantified by calculating the coefficient of variance (CV) for monthly precipitation from April to August (Guo et al., 2012).

$$SDP = \frac{\sqrt{\frac{1}{5}\sum_{i=4}^{8}(P_i - P_{mean})}}{P_{mean}} \quad (13)$$

$$\overline{P} = \frac{1}{5}\sum_{i=4}^{8} P_i \quad (14)$$

Where P_i is the accumulated precipitation of month *i*. P_{mean} is the mean precipitation of the 5 months. A high SDP suggests precipitation is highly concentrated in the growing season. On the contrary, a low SDP suggests precipitation is evenly distributed in the growing season.

To establish the relationships between NPP and GSP, and between NPP and SDP, the partial correlation analysis was used to reflect whether SDP affects NPP variability independent of GSP (Mao et al., 2014). The stepwise regression model was adopted to quantify the relative contribution of GSP and SDP to the temporal variability in NPP (Graham, 2003).

$$r_{xy} = \frac{\sum_{i=1}^{n}(x_i - x_{mean})(y_i - y_{mean})}{\sqrt{\sum_{i=1}^{n}(x_i - x_{mean})^2 \sum_{i=1}^{n}(y_i - y_{mean})^2}} \quad (15)$$

Where r_{xy} is the Pearson correlation coefficient. x_i and y_i represent precipitation variables (GSP or SDP) and annual NPP in the year *i*. x_{mean} and y_{mean} are the multi-year mean values for *x* and *y*.

$$r^*_{xy.z} = \frac{r_{xy} - r_{xz}r_{yz}}{\sqrt{(1-r_{xz}^2)(1-r_{yz}^2)}} \quad (16)$$

Where $r^*_{xy.z}$ is the partial correlation coefficient, showing the relationship between variable *x* and variable *y* after excluding the effect of variable *z*. *y* is NPP. *x* and *z* are two different precipitation variables (GSP or SDP). The T-test was applied to determine the significance level of the correlations of NPP with GSP and SDP. Based on the results of the significance test and the partial correlation analysis, the correlations were classified according to four ranks: significant positive correlation ($r^* \geqslant 0$ and $p \leqslant 0.05$), insignificant positive correlation ($r^* \geqslant 0$ and $p > 0.05$), significant negative correlation ($r^* < 0$ and $p \leqslant 0.05$) and insignificant negative correlation ($r^* < 0$ and $p > 0.05$).

3. Results

3.1 Validations of precipitation and NPP

Fig. 2 showed that the TRMM precipitation data were correlated significantly with the gauge data ($p < 0.001$) at monthly time scales, with the highest correlation coefficient of

0.83 in November and the lowest of 0.69 in February and April. These results suggested that monthly TRMM data achieved reliable spatial distribution of precipitation. In addition, Fig. 3 showed that the correlation coefficients between the observed NPP and the simulated NPP in grasslands and shrublands, respectively, were 0.87 and 0.83, and the CASA NPP had good agreement with the MODIS NPP in forests (r = 0.67) and croplands (r = 0.82). In this study, the CASA model was found to be appropriate for NPP estimation.

Figure 2 here

Figure 3 here

3.2 Annual NPP change

From 2000 to 2013, GSP increased at a rate of 10.6 mm/10 a. Moreover, increases in SDP values at a rate of 0.07/10 a were also observed, which suggested that the distribution of monthly precipitation tended to be more concentrated in the growing season (Fig. 4).

The mean annual NPP was approximately 123.4 g C/m^2, and the coefficient of variance (CV) for annual NPP in the vegetated areas was 6.8% from 2000 to 2013. Fig. 4 showed that annual NPP increased from 2000 to 2004 and changed into a steady phase with minor fluctuations during 2004-2011, and then increased rapidly between 2011 and 2013. Generally, annual NPP has increased at a rate of 1.1 g C·m^{-2}·a^{-1}, with total increases of 11.7% from 2000 to 2013 (p = 0.038).

Regarding annual NPP variability for different land cover types (Fig. 4), the largest mean annual NPP occurred in croplands (250.1 g C/m^2) followed by forests (198.4 g C/m^2), grasslands (120.7 g C/m^2) and shrublands (95.9 g C/m^2). The CV values of annual NPP were higher in grasslands (7.1%) and shrublands (6.9%) than that in forests (4.6%) and croplands (4.2%). Moreover, there were significant increasing trends in annual NPP for grasslands and shrublands, at rates of 1.3 g C·m^{-2}·a^{-1} (13.6% total increases, p = 0.02) and 1.1 g C·m^{-2}·a^{-1} (14.9% total increases, p = 0.005), respectively.

Figure 4 here

Annual NPP trend patterns for 2000-2013 were spatially heterogeneous, but the NPP main trend was increasing (Fig. 5). Most of the vegetated areas (77.6%) showed an increasing trend in annual NPP, and this trend was statistically significant over 18.4% of the area, particularly in the southern Junggar Basin, western Tarim Basin, Hexi Corridor, eastern Tengger Desert, northern Otindag Sandy Land and western Hulun Buir Sandy Land. With regard to areas with significant increases in annual NPP, grassland and shrubland accounted for 53.3% and 40.2% of the areas, respectively (Table 1). However, a decreasing trend in certain regions should not be ignored. Areas with a decreasing trend in annual NPP accounted for only 2.5% the vegetated areas, particularly in the low reaches of Tarim River, and Ili Basin. Shrubland and

grassland accounted for 44% and 32% the areas with significant decreases in annual NPP, respectively (Table 1).

Table 1 here

Figure 5 here

3.3 The effects of GSP and SDP on NPP variability

In this study, the partial correlation coefficients (r^*) of NPP with GSP and SDP were calculated (Table 2). Our results suggested that GSP was positively correlated with NPP in the total vegetated areas ($r^* = 0.93$, $p < 0.001$), after statistically removing the confounding effect of SDP. SDP had a negative effect on NPP in the total vegetated areas ($r^* = -0.79$, $p < 0.001$), after statistically removing the confounding effect of GSP. NPP was closely related to GSP in most of the land cover types (except for forests), with the highest correlation coefficient of 0.92 ($p < 0.001$) observed in grasslands followed by shrublands ($r^* = 0.90$, $p < 0.001$) and croplands ($r^* = 0.69$, $p = 0.01$). In addition to the effect of GSP, SDP exerted a significantly negative effect on NPP in grasslands ($r^* = -0.79$, $p < 0.001$) and shrublands ($r^* = -0.67$, $p = 0.012$), while no strong relationships between SDP and NPP were established in forests and croplands.

Table 2 here

Spatial distributions of the partial correlation coefficients of NPP with GSP and SDP were presented in Fig. 6. From 2000 to 2013, most of the vegetated areas (94.1%) represented a positive correlation between NPP and GSP (Fig. 6a), and 61.7% of the vegetated areas exhibited a statistically significant positive correlation, particularly in the Hexi Corridor, northeastern and southeastern Junggar Basin, eastern Alxa Plateau, Ulanqab Plateau, central Xilingol Plateau and eastern Hulun Buir Plateau. NPP in the lower reaches of Tarim River, and southern Tarim Basin was negatively correlated with GSP, accounting for 5.9% of the vegetated areas (0.3% with a significant correlation). After removing the effect of GSP on plant productivity (Fig. 6b), 77.3% of the vegetated areas showed a negative correlation between NPP and SDP, and 21.5% of the vegetated areas had a statistically significant negative correlation, particularly in the Junggar Basin, Hexi Corridor, eastern Alxa Plateau, Ulanqab Plateau and Xilingol Plateau. NPP was positively correlated with SDP in the lower reaches of Tarim River, northern Junggar Basin, eastern Otindag Sandy Land and western Hulun Buir Sandy Land, accounting for 22.7% of the vegetated areas (1.6% with a significant correlation).

Figure 6 here

The stepwise regression model was employed to quantify the relative contribution of GSP and SDP to NPP variability for different land cover types (Table 2). Our results suggested that

GSP was the main driving factor of NPP variability for grasslands, shrublands, croplands and the total vegetated areas, with a contribution of 63.8%, 65.4%, 37.8% and 66.7%, respectively. NPP responded to SDP change rapidly without any change to GSP. SDP partly explained 22.8%, 15.5% and 21% of the variability in NPP for grasslands, shrublands and the total vegetated areas, respectively. However, GSP and SDP had no dramatic impacts on forest NPP.

4. Discussion

4.1 The response of NPP to GSP

We found that annual NPP in the arid region of northern China increased significantly from 2000 to 2013 (Fig. 5). This result had consistency with previous studies. For instance, An et al. (2014) found that northern China had general increases in greenness over the period of 1982–2011 using AVHRR GIMMS and MODIS NDVI data. Mao et al. (2014) suggested that there were slight increases in annual aboveground grassland NPP in northern China between 2000 and 2011. Zhang et al. (2014) demonstrated that the northern China's grassland had a net carbon uptake of 158 ± 25 g C/m^2 over the growing season from 2000 to 2010 with the mean regional net ecosystem production estimate of 126 Tg C.

Precipitation was regarded as the most crucial factor that drove NPP variability in arid regions (Knapp et al., 2008; Potter et al., 1999; Zeppel et al., 2014). It was widely established that NPP increased with increasing mean annual precipitation in arid and semiarid regions (Knapp and Smith, 2001; Ma et al., 2008; Muldavin et al., 2008). Based on a meta-analysis of experimental manipulation, NPP increased with increasing precipitation and vice versa (Wu et al., 2011). In this study, significant positive correlations between GSP and NPP were found in most of the vegetated areas (Fig. 6a). GSP explained much of the variability in NPP with a contribution of almost 67% (Table 2). Over the period of 2000-2013, GSP increased at a rate of 10.6 mm/10 a (Fig. 4). Precipitation had a direct influence on soil moisture (Weltzin et al., 2003). Thus, a significant increasing trend in NPP might be attributed to the impact of soil water replenishment on root activity, plant water status and photosynthesis (Fay et al., 2008).

We also found that a 30% increase in precipitation increased NPP by 20%; however, a 30% decrease in precipitation decreased NPP by 12%, which implied that NPP responded more strongly to higher precipitation than lower precipitation (Fig. 4). A possible reason for this unique phenomenon was that decreased precipitation caused serious soil water deficits, and photosynthesis was progressively constrained as stomatal closure affected not only the CO_2 diffusion into chloroplasts but also key photosynthetic pathways, like photophosphorylation and ribulose 1,5-biphosphate regeneration (Huxman et al., 2004). Severe water limitation could boost photosynthesis consumption to relieve water stress and to support individual development (Reyer et al., 2013). However, higher precipitation might lead to dramatic increases in NPP due to open water use strategies and compensatory effects among species as

plant community generally had higher biodiversity in wet seasons than in dry seasons (Guo et al., 2012).

Responses of NPP to precipitation anomalies were likely to vary for different land cover types. We found that the greatest inter-annual variability in annual NPP occurred in grasslands, with forests the least variable (Table 1). No relationships between precipitation and forest NPP were found, and grassland NPP was more strongly correlated with precipitation variability than any other land cover type (Table 2). Most of the forests were able to withstand water deficits as they might have access to water contained in the deep soil layers (Ogle and Reynolds, 2004). Herbaceous plants in arid regions usually had high production potential, which was characterized by their immediate responses to precipitation pulses through germination, growing and producing large quantities of seeds (Holmgren et al., 2006).

The Palmer Drought Severity Index (PDSI) measured soil wetness (positive values) and dryness (negative values) based a soil water balance equation (Dai, 2013). The region with negative values of mean annual PDSI suggested a dry environment, whereas the region with positive values indicated a more humid environment. We found that NPP was more positively related with precipitation variability in very dry areas; however, NPP was less responsive to precipitation variability in more humid areas (Fig. 7). Plant species in extremely arid environments might evolve special physiological and morphological characteristics, which allowed them to rapidly adapt to variations in water availability (Vicente-Serrano et al., 2013). For example, Xu et al. (2006) found that two non-phreatophyte desert shrubs (*Haloxylon ammodendron* and *Reaumuria soongorica*) were able to maintain normal photosynthesis within a wide range of plant water status due to their effective morphological adjustment in both the root and shoot systems. The low NPP-Precipitation correlations in more humid areas suggested that even below average precipitation was sufficient to maintain photosynthetic activities as antecedent soil moisture might increase water availability and partially dampen the relationship between NPP and precipitation anomalies (Gessner et al., 2013). Roerink et al. (2003) also found that vegetation displayed the high sensitivity to precipitation changes in dry areas, almost no sensitivity in moderately humid areas.

Figure 7 here

4.2 The response of NPP to SDP

Empirical studies demonstrated that there were lags decoupling NPP and precipitation inputs. For example, Li et al. (2013) found that increased precipitation during the previous autumn and winter enhanced vegetation growth in the growing season. As evapotranspiration was limited in autumn and winter over arid and semiarid regions, precipitation could accumulate and infiltrate into deep soil horizons, making water available to plant growth

during the spring-summer growing season (Weltzin et al., 2003). In this study, NPP was closely related to GSP; however, we failed to detect a relationship between previous-year precipitation and current-year production (Fig. 4). Precipitation decreases would not be detrimental to NPP unless intense soil water deficits occurred (Zeppel et al., 2014).

Higher precipitation intensity was predicted to cause deeper penetration of soil water into the profile and less proportional loses to evaporation; however, more extended dry intervals between events resulted in longer periods of soil moisture depletion in the upper layers (Knapp et al., 2008). Grasses (or other herbaceous plants) were relatively shallow-rooted and extensively utilized superficial water (Knapp and Smith, 2001). In this study, SDP was negatively correlated with grassland NPP (Table 2). Our study supported the two-layer soil water-partitioning hypothesis, which suggested that increased precipitation concentration would decrease soil moisture in the surface layers, and hence grassland NPP. On the contrary, the survival of deep-rooted plants, such as shrubs, depended mainly on soil moisture in the deeper layers. Thus, increases in the number of larger precipitation events ($>$5 mm) would favour shrub establishment and growth (Schwinning and Sala, 2004). Nevertheless, we found that SDP was negatively correlated with shrubland NPP (Table 2), which suggested that increased precipitation concentration might depress the growth of the shrublands. The persistence of the water deficit could play a key role in determining the response of shrubland NPP to drought (Vicente-Serrano et al., 2013). Recent studies reported that deep-rooted plants were not always superior to shallow-rooted plants in their ability to tolerate drought stress due to the diversity of rooting habits among species (Xu et al., 2006; West et al., 2012). Moreover, antecedent soil moisture was a critical factor as it might diminish or amplify the effect of precipitation pulses on plant production. For instance, when deep horizons were relatively dry, shrubs exploited surface soil water gained from recent rains (Schwinning et al., 2002). This paper revealed a negative correlation between NPP and precipitation anomalies in the low reaches of Tarim River (Fig. 5). Human activities, such as overgrazing and overexploitation of water resources, might cause the degradation of natural vegetation and act as dominant factors in desertification development regardless of increased precipitation (Zhou et al., 2015). Furthermore, no relationships between SDP and cropland NPP were found (Table 2). Human activities could mediate cropland NPP responses to precipitation changes through irrigation and fertilizer utilization (Valipour, 2015a).

5. Conclusions

Given the importance of NPP as an indicator of ecosystem function, as well as its role in global carbon cycle, developing the relationship between NPP and altered precipitation regimes in arid regions may improve our knowledge of vegetation vulnerability to climate change. Our results suggested that NPP has significantly increased by 11.7% in the arid

region of northern China since 2000. Responses of NPP to growing season precipitation and its seasonal distribution varied for different land cover types. Grassland and shrubland displayed a higher temporal variability in NPP and were more responsive to variability in precipitation than forests and croplands. NPP increased with increasing precipitation, whereas increased precipitation concentration decreased NPP. Growing season precipitation and seasonal distribution of precipitation were major drivers of NPP variability in the arid region of northern China, which accounted approximately 67% and 21% of the variability in NPP. Meanwhile, how NPP responded to alterations in growing season precipitation and its seasonal distribution might be partly dependent on the plant functional trait, antecedent soil moisture and anthropogenic activities. These factors could illustrate regional differences in the relationship between NPP and altered precipitation regimes.

Acknowledgements

This research was funded by the 100-talents Program of the Chinese Academy of Sciences, and the National Natural Science Foundation of China (Nos. 41371101 and 41530750). We thank two anonymous referees for their detailed comments that improve this paper substantially. We also thank Dr. Mihretab G. Ghebrezgabher for his help in English editing.

References

An, Y., Gao, W., Gao, Z., 2014. Characterizing land condition variability in Northern China from 1982 to 2011. Environ. Earth Sci. 72, 663-676.

Baez, S., Collins, S.L., Pockman, W.T., Johnson, J.E., Small, E.E., 2013. Effects of experimental rainfall manipulations on Chihuahuan Desert grassland and shrubland plant communities. Oecologia 172, 1117-1127.

Bates, J.D., Svejcar, T., Miller, R.F., Angell, R.A., 2006. The effects of precipitation timing on sagebrush steppe vegetation. J. Arid. Environ. 64, 670-697.

Chen, B., Zhang, X., Tao, J., Wu, J., Wang, J., Shi, P., Zhang, Y., Yu, C., 2014. The impact of climate change and anthropogenic activities on alpine grassland over the Qinghai-Tibet Plateau. Agric. For. Meteorol. 189, 11-18.

Chen, J., Jönsson, P., Tamura, M., Gu, Z., Matsushita, B., Eklundh, L., 2004. A simple method for reconstructing a high-quality NDVI time-series data set based on the Savitzky−Golay filter. Remote Sens. Environ. 91, 332-344.

Craine, J.M., Nippert, J.B., Elmore, A.J., Skibbe, A.M., Hutchinson, S.L., Brunsell, N.A., 2012. Timing of climate variability and grassland productivity. Proc. Natl. Acad. Sci. U. S. A. 109, 3401-3405.

Dai, A., 2013. Increasing drought under global warming in observations and models. Nat. Clim. Chang. 3, 52-58.

Easterling, D.R., Meehl, G.A., Parmesan, C., Changnon, S.A., Karl, T.R., Mearns, L.O., 2000. Climate extremes: observations, modeling, and impacts. Science 289, 2068-2074.

Fang, J.Y., Piao, S.L., Tang, Z.Y., Peng, C.H., Wei, J., 2001. Interannual variability in net primary production and precipitation. Science 293, 1723a.

Fay, P.A., Kaufman, D.M., Nippert, J.B., Carlisle, J.D., Harper, C.W., 2008. Changes in grassland ecosystem function due to extreme rainfall events: implications for responses to climate change. Glob. Change Biol. 14, 1600-1608.

Fensholt, R., Rasmussen, K., Nielsen, T.T., Mbow, C., 2009. Evaluation of earth observation

based long term vegetation trends-Intercomparing NDVI time series trend analysis consistency of Sahel from AVHRR GIMMS, Terra MODIS and SPOT VGT data. Remote Sens. Environ. 113, 1886-1898.

Gessner, U., Naeimi, V., Klein, I., Kuenzer, C., Klein, D., Dech, S., 2013. The relationship between precipitation anomalies and satellite-derived vegetation activity in Central Asia. Glob. Planet. Change 110, 74-87.

Graham, M.H., 2003. Confronting multicollinearity in ecological multiple regression. Ecology 84, 2809-2815.

Guo, Q., Hu, Z., Li, S., Li, X., Sun, X., Yu, G., 2012. Spatial variations in aboveground net primary productivity along a climate gradient in Eurasian temperate grassland: effects of mean annual precipitation and its seasonal distribution. Glob. Change Biol. 18, 3624-3631.

Hancock, P.A., Hutchinson, M.F., 2006. Spatial interpolation of large climate data sets using bivariate thin plate smoothing splines. Environ. Modell. Softw. 21, 1684-1694.

Heisler-White, J.L., Knapp, A.K., Kelly, E.F., 2008. Increasing precipitation event size increases aboveground net primary productivity in a semi-arid grassland. Oecologia 158, 129-140.

Holmgren, M., Stapp, P., Dickman, C.R., Gracia, C., Graham, S., Gutierrez, J.R., Hice, C., Jaksic, F., Kelt, D.A., Letnic, M., Lima, M., Lopez, B.C., Meserve, P.L., Milstead, W.B., Polis, G.A., Previtali, M.A., Michael, R., Sabate, S., Squeo, F.A., 2006. Extreme climatic events shape arid and semiarid ecosystems. Front. Ecol. Environ. 4, 87-95.

Hoover, D.L., Knapp, A.K., Smith, M.D., 2014. Resistance and resilience of a grassland ecosystem to climate extremes. Ecology 95, 2646-2656.

Huxman, T.E., Snyder, K.A., Tissue, D., Leffler, A.J., Ogle, K., Pockman, W.T., Sandquist, D.R., Potts, D.L., Schwinning, S., 2004. Precipitation pulses and carbon fluxes in semiarid and arid ecosystems. Oecologia 141, 254-268.

Kunkel, K.E., Andsager, K., Easterling, D.R., 1999. Long-term trends in extreme precipitation events over the conterminous United States and Canada. J. Clim. 12, 2515-2527.

Knapp, A.K., Beier, C., Briske, D.D., Classen, A.T., Luo, Y., Reichstein, M., Smith, M.D., Smith, S.D., Bell, J.E., Fay, P.A., Heisler, J.L., Leavitt, S.W., Sherry, R., Smith, B., Weng, E., 2008. Consequences of more extreme precipitation regimes for terrestrial ecosystems. Bioscience 58, 811-821.

Knapp, A.K., Smith, M.D., 2001. Variation among biomes in temporal dynamics of aboveground primary production. Science 291, 481-484.

Li, F., Zhao, W., Liu, H., 2013. The response of aboveground net primary productivity of desert vegetation to rainfall pulse in the temperate desert region of Northwest China. PLoS One 8, e73003.

Ma, M.G., Frank, V., 2006. Interannual variability of vegetation cover in the Chinese Heihe river Basin and its relation to meteorological parameters. Int. J. Remote Sens. 27, 3473-3486.

Ma, W., Yang, Y., He, J., Hui, Z., Fang, J., 2008. Above- and belowground biomass in relation to environmental factors in temperate grasslands, Inner Mongolia. Sci. China-Life Sci. 51, 263-270.

Mao, D., Wang, Z., Li, L., Ma, W., 2014. Spatiotemporal dynamics of grassland aboveground net primary productivity and its association with climatic pattern and changes in Northern China. Ecol. Indic. 41, 40-48.

Muldavin, E.H., Moore, D.I., Collins, S.L., Wetherill, K.R., Lightfoot, D.C., 2008. Aboveground net primary production dynamics in a northern Chihuahuan Desert ecosystem. Oecologia 155, 123-132.

Myneni, R.B., Williams, D.L., 1994. On the relationship between FAPAR and NDVI. Remote Sens. Environ. 49, 200-211.

Noy-Meir, I., 1973. Desert ecosystems: environment and producers. Annu. Rev. Ecol. Evol.

Syst. 4, 25 - 51.
Ogle, K., Reynolds, J.F., 2004. Plant responses to precipitation in desert ecosystems: integrating functional types, pulses, thresholds, and delays. Oecologia 141, 282-294.
Pettorelli, N., Chauvenet, A.L.M., Duffy, J.P., Cornforth, W.A., Meillere, A., Baillie, J.E.M., 2012. Tracking the effect of climate change on ecosystem functioning using protected areas: Africa as a case study. Ecol. Indic. 20, 269-276.
Potter, C.S., Klooster, S., Brooks, V., 1999. Interannual variability in terrestrial net primary production: Exploration of trends and controls on regional to global scales. Ecosystems 2, 36-48.
Rahimi, S., Sefidkouhi, M.A.G., Raeini-Sarjaz, M., Valipour, M., 2015. Estimation of actual evapotranspiration by using MODIS images (a case study: Tajan catchment). Arch. Agron. Soil Sci. 61, 695-709.
Reyer, C.P.O., Leuzinger, S., Rammig, A., Wolf, A., Bartholomeus, R.P., Bonfante, A., de Lorenzi, F., Dury, M., Gloning, P., Abou Jaoude, R., Klein, T., Kuster, T.M., Martins, M., Niedrist, G., Riccardi, M., Wohlfahrt, G., de Angelis, P., de Dato, G., Francois, L., Menzel, A., Pereira, M., 2013. A plant's perspective of extremes: terrestrial plant responses to changing climatic variability. Glob. Change Biol. 19, 75-89.
Robertson, T.R., Bell, C.W., Zak, J.C., Tissue, D.T., 2009. Precipitation timing and magnitude differentially affect aboveground annual net primary productivity in three perennial species in a Chihuahuan Desert grassland. New Phytol. 181, 230-242.
Roerink, G.J., Menenti, M., Soepboer, W., Su, Z., 2003. Assessment of climate impact on vegetation dynamics by using remote sensing. Phys. Chem. Earth 28, 103-109.
Schimel, D.S., House, J.I., Hibbard, K.A., Bousquet, P., Ciais, P., Peylin, P., Braswell, B.H., Apps, M.J., Baker, D., Bondeau, A., Canadell, J., Churkina, G., Cramer, W., Denning, A.S., Field, C.B., Friedlingstein, P., Goodale, C., Heimann, M., Houghton, R.A., Melillo, J.M., Moore, B., Murdiyarso, D., Noble, I., Pacala, S.W., Prentice, I.C., Raupach, M.R., Rayner, P.J., Scholes, R.J., Steffen, W.L., Wirth, C., 2001. Recent patterns and mechanisms of carbon exchange by terrestrial ecosystems. Nature 414, 169-172.
Schwinning, S., Davis, K., Richardson, L., Ehleringer, J.R., 2002. Deuterium enriched irrigation indicates different forms of rain use in shrub/grass species of the Colorado Plateau. Oecologia 130, 345-355.
Schwinning, S., Sala, O.E., 2004. Hierarchy of responses to resource pulses in arid and semi-arid ecosystems. Oecologia 141, 211-220.
Smith, M.D., 2011. The ecological role of climate extremes: current understanding and future prospects. J. Ecol. 99, 651-655.
Sun, Q., Feng, X., Ge, Y., Li, B., 2015. Topographical effects of climate data and their impacts on the estimation of net primary productivity in complex terrain: A case study in Wuling mountainous area, China. Ecol. Inform. 27, 44-54.
Taddei, R., 1997. Maximum value interpolated (MVI): A Maximum Value Composite method improvement in vegetation index profiles analysis. Int. J. Remote Sens. 18, 2365-2370.
Valipour, M., 2014. Future of the area equipped for irrigation. Arch. Agron. Soil Sci. 60, 1641-1660.
Valipour, M., 2015a. A comprehensive study on irrigation management in Asia and Oceania. Arch. Agron. Soil Sci. 61, 1247-1271.
Valipour, M., 2015b. Evaluation of radiation methods to study potential evapotranspiration of 31 provinces. Meteorol. Atmos. Phys. 127, 289-303.
Valipour, M., 2015c. Investigation of Valiantzas' evapotranspiration equation in Iran. Theor. Appl. Climatol. 121, 267-278.
Vicente-Serrano, S.M., Gouveia, C., Julio Camarero, J., Begueria, S., Trigo, R., Lopez-Moreno, J.I., Azorin-Molina, C., Pasho, E., Lorenzo-Lacruz, J., Revuelto, J., Moran-

Tejeda, E., Sanchez-Lorenzo, A., 2013. Response of vegetation to drought time-scales across global land biomes. Proc. Natl. Acad. Sci. U. S. A. 110, 52-57.

Walter, H., 1971. Natural savannahs as a transition to the arid zone, in: Walter, H. (Eds.), Ecology of tropical and subtropical vegetation. Oliver and Boyd., Edinburgh, pp. 238–265.

Weltzin, J.F., Loik, M.E., Schwinning, S., Williams, D.G., Fay, P.A., Haddad, B.M., Harte, J., Huxman, T.E., Knapp, A.K., Lin, G.H., Pockman, W.T., Shaw, M.R., Small, E.E., Smith, M.D., Smith, S.D., Tissue, D.T., Zak, J.C., 2003. Assessing the response of terrestrial ecosystems to potential changes in precipitation. Bioscience 53, 941-952.

West, A.G., Dawson, T.E., February, E.C., Midgley, G.F., Bond, W.J., Aston, T.L., 2012. Diverse functional responses to drought in a Mediterranean-type shrubland in South Africa. New Phytol. 195, 396-407.

Wu, Z., Dijkstra, P., Koch, G.W., Penuelas, J., Hungate, B.A., 2011. Responses of terrestrial ecosystems to temperature and precipitation change: a meta-analysis of experimental manipulation. Glob. Change Biol. 17, 927-942.

Xu, H., Li, Y., 2006. Water-use strategy of three central Asian desert shrubs and their responses to rain pulse events. Plant Soil 285, 5-17.

Yang, Y., Fang, J., Ma, W., Guo, D., Mohammat, A., 2010. Large-scale pattern of biomass partitioning across China's grasslands. Glob. Ecol. Biogeogr. 19, 268-277.

Yu, D.Y., Shi, P.J., Han, G.Y., Zhu, W.Q., Du, S.Q., Xun, B., 2011. Forest ecosystem restoration due to a national conservation plan in China. Ecol. Eng. 37, 1387-1397.

Zeppel, M.J.B., Wilks, J.V., Lewis, J.D., 2014. Impacts of extreme precipitation and seasonal changes in precipitation on plants. Bioscience 11, 3083-3093.

Zhang, L., Guo, H., Jia, G., Wylie, B., Gilmanov, T., Howard, D., Ji, L., Xiao, J., Li, J., Yuan, W., Zhao, T., Chen, S., Zhou, G., Kato, T., 2014. Net ecosystem productivity of temperate grasslands in northern China: An upscaling study. Agric. For. Meteorol. 184, 71-81.

Zhao, F., Xu, B., Yang, X., Jin, Y., Li, J., Xia, L., Chen, S., Ma, H., 2014. Remote sensing estimates of grassland aboveground biomass based on MODIS net primary productivity (NPP): A case study in the Xilingol grassland of northern China. Remote Sens. 6, 5368-5386.

Zhao, M., Heinsch, F.A., Nemani, R.R., Running, S.W., 2005. Improvements of the MODIS terrestrial gross and net primary production global data set. Remote Sens. Environ. 95, 164-176.

Zhou, W., Gang, C., Zhou, F., Li, J., Dong, X., Zhao, C., 2015. Quantitative assessment of the individual contribution of climate and human factors to desertification in northwest China using net primary productivity as an indicator. Ecol. Indic. 48, 560-569.

Zhu, W.Q., Pan, Y.Z., He, H., Yu, D.Y., Hu, H.B., 2006. Simulation of maximum light use efficiency for some typical vegetation types in China. Chin. Sci. Bull. 51, 457-463.

Table caption

Table 1

The proportions of areas with different NPP trends for different land cover types from 2000 to 2013.

Table 2

The partial correlation coefficients of annual NPP with growing season precipitation (GSP) and seasonal distribution of precipitation (SDP). The contributions of GSP and SDP to NPP variability are assessed for different land cover types by using the stepwise regression model.

Table 1

Variation types	Forest		Shrubland		Grassland		Cropland	
	A	B	A	B	A	B	A	B
Significant increase	10.5	0	18.7	7.4	18.2	9.8	18.6	1.2
Insignificant increase	42.2	0.1	61.2	24.1	60.9	32.7	33.5	2.2
Significant decrease	7.2	0	2.7	1.1	1.5	0.8	8.6	0.6
Insignificant decrease	40.0	0.1	17.4	6.9	19.4	10.4	39.3	2.6
Sum	100	0.2	100	39.5	100	53.7	100	6.6

A is the percentage in this land cover type.

B is the percentage in the total vegetated areas.

Table 2

Land cover type	GSP			SDP		
	r^*	SS(%)	p	r^*	SS(%)	p
Forest	0.45	—	0.126	-0.17	—	0.576
Shrubland	0.90	65.4	＜0.001	-0.67	15.5	0.012
Grassland	0.92	63.8	＜0.001	-0.79	22.8	＜0.001
Cropland	0.69	37.8	0.01	-0.41	—	0.164
Total vegetated areas	0.93	66.7	＜0.001	-0.79	21.0	＜0.001

r^* is the partial correlation coefficient.

SS denotes model explanation.

Figure caption

Fig. 1 Location of the study area and spatial distributions of meteorological stations, sample sites and land cover types in the arid region of northern China. The insert graph (Panel a) shows the area percentage of each land cover type to the total study area.

Fig. 2 Scatter plots of the areal average precipitation from TRMM and precipitation gauges data at monthly time scales.

Fig. 3 Comparisons of the CASA and MODIS NPP estimates in forests (a) and croplands (b), and the relationships between the measured NPP and the simulated NPP in grasslands (c) and shrublands (d).

Fig. 4 Inter-annual variations in NPP, growing season precipitation (GSP) and seasonal distribution of precipitation (SDP) for different land cover types from 2000 to 2013. The dash line shows a significant linear trend in annual NPP at a 95% confidence level.

Fig. 5 Trends in annual NPP with a statistical significance test at the 5% level from 2000 to 2013. The inset graphs represent the area frequency distribution in each class of NPP change rates.

Fig. 6 Spatial distributions of the partial correlation levels of annual NPP with growing season precipitation (GSP) and seasonal distribution of precipitation (SDP). The inset graphs in each panel of the figure (Panel a & Panel b) represent the area percentage of each correlation level at 5% significance to the total vegetated areas.

Fig. 7 Relationships between the NPP-Precipitation correlation coefficient and the annual Palmer Drought Severity Index (PDSI). The boxes show the 25^{th}, 50^{th} and 75^{th} percentiles, and the whiskers show the 5^{th} and 95^{th} percentiles.

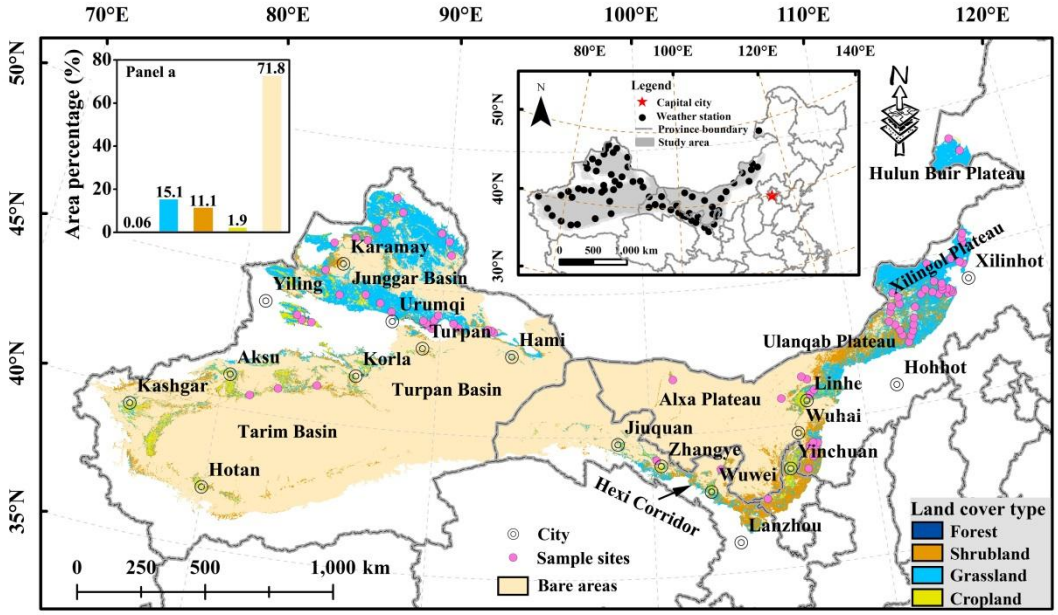

Figure 1

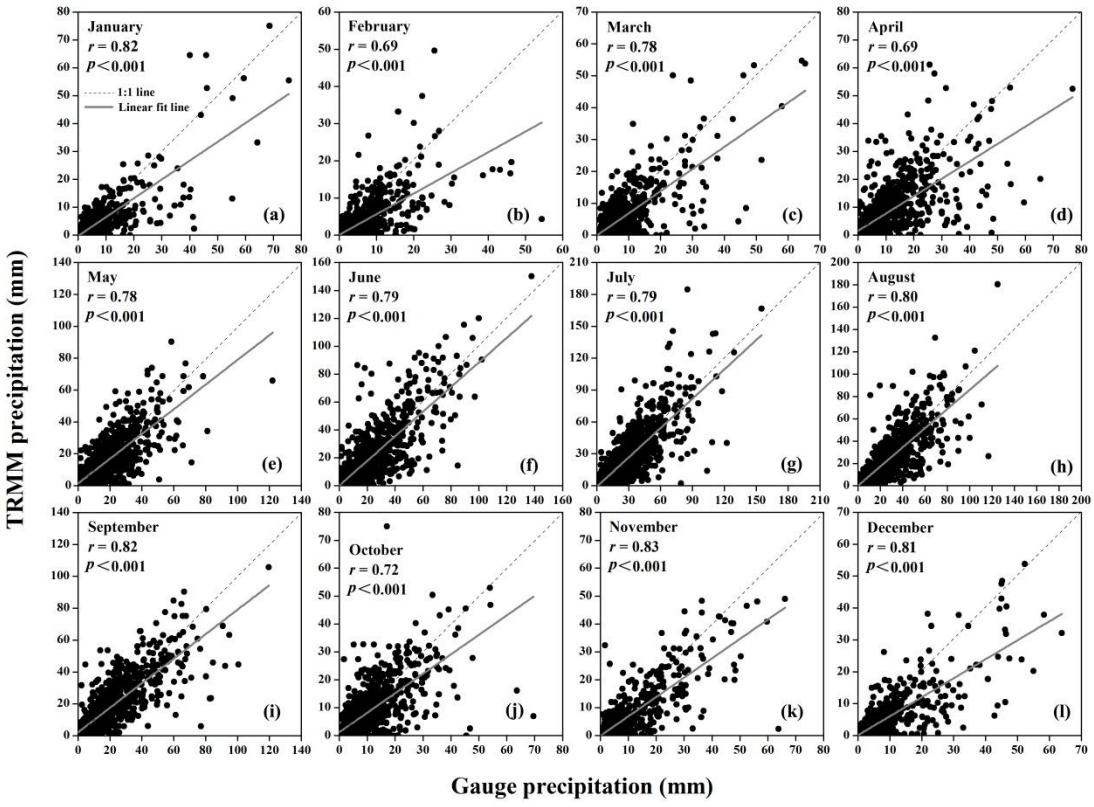

Figure 2

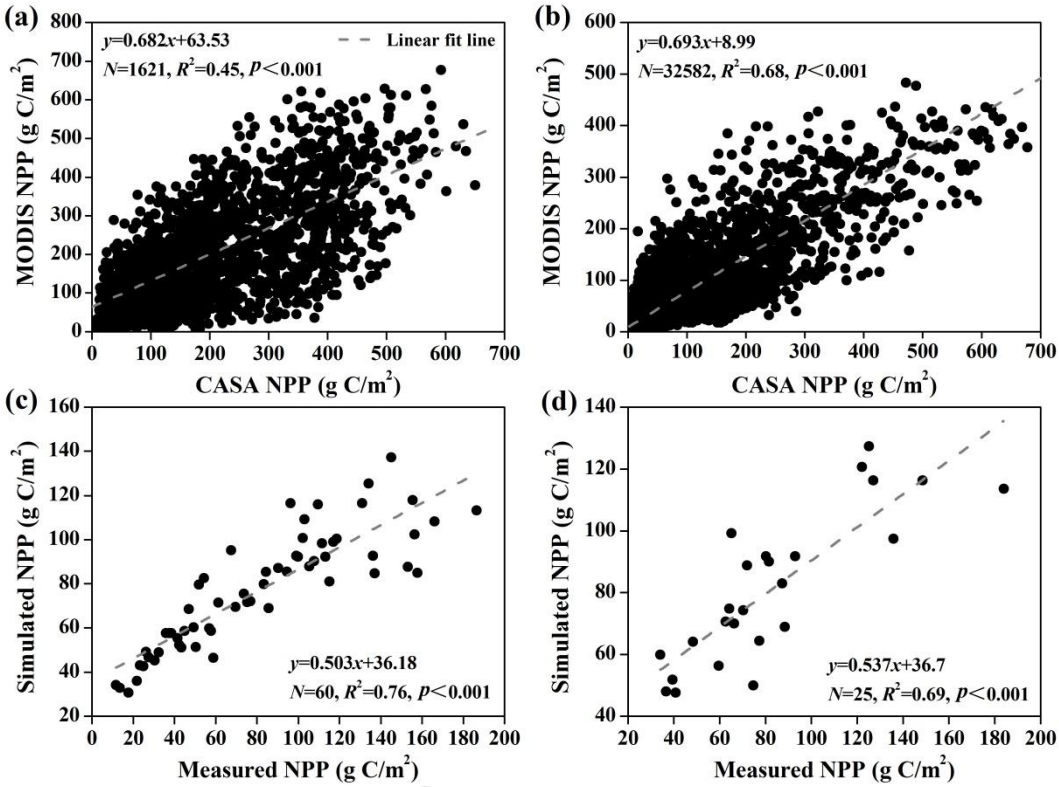

Figure 3

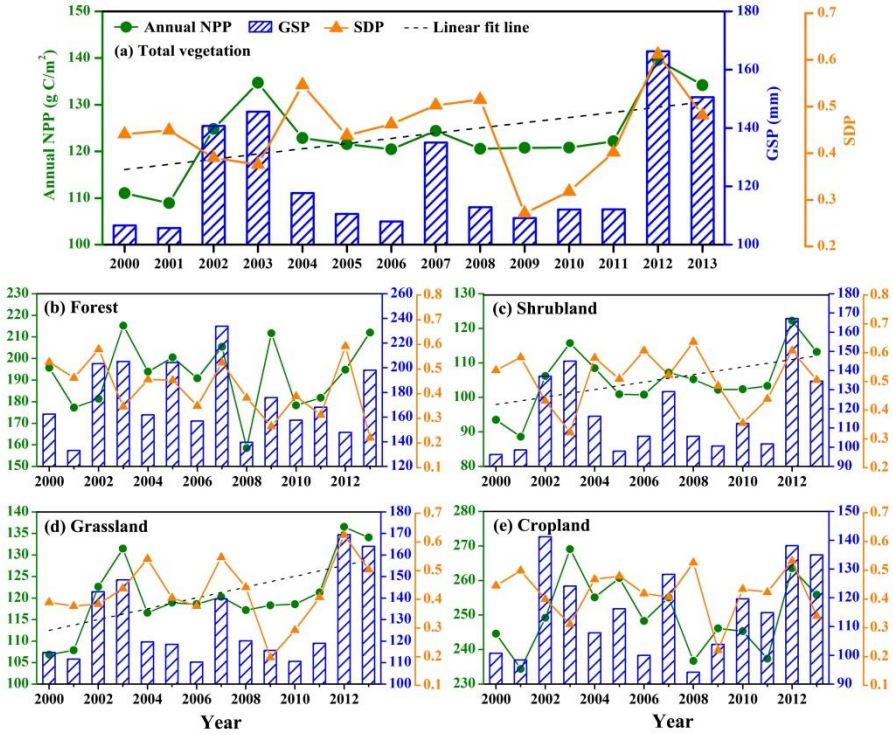

Figure 4

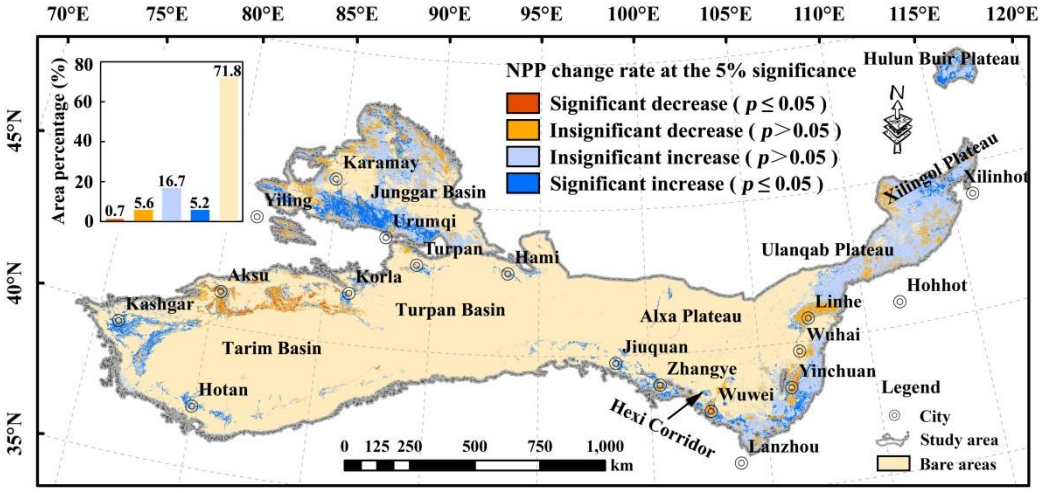

Figure 5

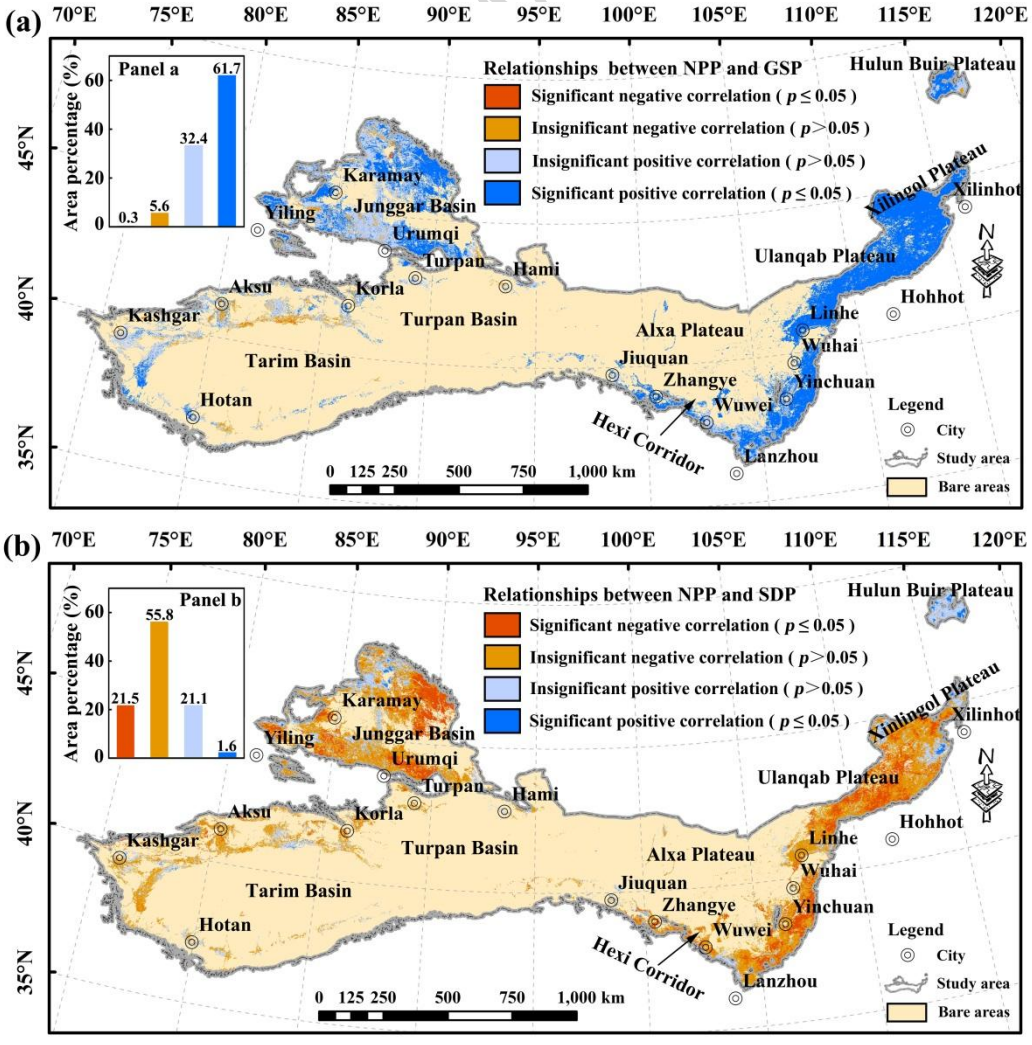

Figure 6

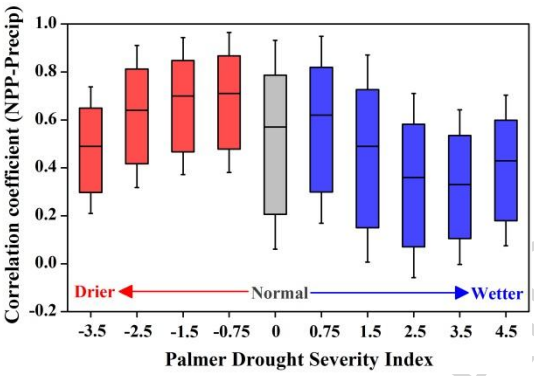

Figure 7

Highlights

- **How altered precipitation regimes influence terrestrial ecosystem function in arid regions is uncertain.**
- **We estimated annual net primary productivity of different land cover types through the CASA (Carnegie–Ames–Stanford Approach) model.**
- **The effects of growing season precipitation and its seasonal distribution on NPP variability were quantified.**
- **The paper has implications for assessing vegetation vulnerability to future scenarios of more extreme intra-annual precipitation patterns.**